These equations shows that the kinetics of x and y effect each other, i.e., the concentrations of CTA^+ and A^- near the interface are mutually dependent. Equations 1 and 2 represent the kinetics of diffusion of picric acid from the bulk organic phase and of diffusion of CTAB from the bulk aqueous phase toward the interface, respectively. The last term in eq 3 and 4 implies the "co-operative" behavior between CTA^+ ions in step III (Hill approximation).[11] The parameters chosen tentatively for computation in Figure 2 are $y_{min} = 0.4$, $y_{max} = 0.8$, $\alpha = 0.3$, $\beta = 2$, $c = 0.25$, $\gamma = 2$, $\delta = 30$, $\theta = 2$, and $n = 3$. (Numerical calculations were carried out with use of a Runge-Kutta approximation on a NEC PC-8800 microcomputer.)

In spite of the simplicity of our model, the simulated results reproduce the experimental trend well, as shown in Figure 2. The difference in concentrations of CTA^+ and A^- near the interface may correlate with the electrical potential between the two phases. Indeed the calculated variation of $[x - y]$ corresponds well to that of the electrical potential. The pH value of the aqueous phase may depend on several complicated factors, such as the concentrations of CTA^+ and Br^- and also the concentration and shape of the micells of CTA^+. Accordingly, explanation of the variation of pH is more complicated and difficult than that of variation of the electrical potential. However, it is interesting that the manner of the calculated change of $[y]$ is quite similar to that of pH, as shown in Figure 2.

Our model is too simple to allow discussion of experimental trend quantitatively, but the correspondence of experimental and calculated results suggests its validity. Further experimental and theoretical studies on the oscillatory phenomena are in progress in our laboratory.[12]

Acknowledgment. The authors wish to thank Professor T. Ota for encouragement. This work was supported in part by a Grant-in-Aid for Scientific Research to K.Y. (No. 57750716) from the Mini ry of Education, Science and Culture of Japan.

Registry No. CTAB, 57-09-0; picric acid, 88-89-1; 1-nitropropane, 108-03-2; 2-nitropropane, 79-46-9.

(12) Yoshikawa, K.; Matsubara, Y. *Biophys. Chem.* **1983**, *17*, 183–185.

Matrix Isolation Studies of Nucleic Acid Constituents. 1. Infrared Spectra of Uracil Monomers

M. Szczesniak, M. J. Nowak, H. Rostkowska, K. Szczepaniak,* W. B. Person,*† and D. Shugar‡

Contribution from the Institute of Physics, Polish Academy of Sciences, Al. Lotnikow 32/46, 02-668 Warsaw, Poland. *Received March 30, 1983*

Abstract: Results of infrared studies of uracil and its N_1,N_3-dideuterated homologue isolated in argon and nitrogen matrices are presented and discussed in terms of normal modes predicted by quantum-mechanical calculations. The effects on the spectrum of N-deuteration and of the interaction between the isolated molecule and the matrix are discussed. The quantum-mechanical calculations are used to make a reasonably reliable first assignment of absorption bands to all the normal modes for the matrix-isolated uracil molecule. The wavenumbers and relative intensities for the absorption bands for the isolated molecule are related to those reported previously for uracil in the solid phase but differ significantly from them.

Introduction

For a proper interpretation of the vibrational spectra of nucleic acids in biophysical research, it is essential first to obtain, and then to understand, the spectra for the isolated noninteracting molecules. By studying the spectral changes which occur from the isolated molecule to molecules placed in more and more strongly interacting environments, one may hope to interpret the vibrational spectrum and also to obtain information about the interacting environment of such molecules in truly biological conditions. Although the vibrational spectra of uracils have been extensively investigated in solutions and in the solid state (e.g., ref 1 and 2), the analyses are complicated by intermolecular hydrogen bonding and/or interactions with polar solvents, or by the low solubility in nonpolar solvents. In the vapor phase[3-5] rotational broadening of the bands complicates the analyses of the spectra of the monomeric species.

Matrix isolation spectroscopy provides a unique method for study of vibrational spectra of monomeric molecules under conditions where interaction between molecules, and their rotational motions, are minimized.[6-8] This procedure results in drastic sharpening of the absorption bands, so that bands which overlap in the spectra of the vapor, solution, or solid may often be readily resolved in the spectrum of the matrix. Although some secondary effects may result from the matrix, the infrared spectra of species isolated in rare gas matrices correspond closely to the pure vibrational spectra for molecules in the gas phase. Hence, these results are preferred for comparison with theoretically predicted vibrational spectra.

In a continuation of studies[5] on 2(4)-dioxopyrimidines using matrix isolation infrared spectroscopy, we report here the infrared spectra of uracil and its N_1,N_3-dideuterated homologue. We present the infrared spectrum for the isolated uracil molecule dilute in an argon matrix and its modification in a nitrogen matrix. The

†Department of Chemistry, University of Florida, Gainesville, FL 32611.
‡Institute of Biochemistry and Biophysics, Polish Academy of Sciences, ul. Rakowiecka 36, 02-532 Warsaw, Poland.

(1) H. Susi and J. S. Ard, *Spectrochim. Acta, Part A*, **27**, 1549 (1971).
(2) K. A. Hartman, R. C. Lord, and G. J. Thomas, Jr., in "Physicochemical Properties of Nucleic Acids", Vol. 2, J. Duchesne, Ed., Academic Press, London, 1973, and references given there.
(3) M. J. Nowak, K. Szczepaniak, A. Barski, and D. Shugar. *Z. Naturforsch. C*, **33**, 876 (1978).
(4) M. J. Nowak, K. Szczepaniak, A. Barski, and D. Shugar, *J. Mol. Struct.*, **47** (1980).
(5) M. J. Nowak, Ph.D. Thesis, University of Warsaw, 1979.
(6) H. E. Hallam, Ed., "Vibrational Spectroscopy of Trapped Species", Wiley, London, 1973.
(7) S. Cradock and A. J. Hinchliffe, "Matrix Isolation", Cambridge University Press, London, 1975.
(8) A. J. Barnes, W. J. Orville-Thomas, A. Müller, and R. Gaufres, Eds., "Matrix Isolation Spectroscopy", NATO ASI Ser. C, Vol. 76, Reidel Publishing Co., Dordrecht, Netherlands, 1981.

0002-7863/83/1505-5969$01.50/0

results for concentrated matrix and for pure solid films will be presented and discussed elsewhere.[9] The results presented here provide the infrared spectrum for the undistorted uracil molecule, and deviations from this spectrum will measure its interactions with the environment. Such studies on a series of related molecules with different substituents[10,11] can be expected to furnish useful information about the infrared spectroscopic behavior of uracil (and other nucleic base residues) in nucleic acids.

Experimental Section

Uracil was a product of Waldhof-Pharmacia (Stuttgart, GFR), and the N_1,N_3-dideuterated analogue was obtained by repeated exchange with D_2O until the NH stretching band intensity had decreased to less than 1% of the ND stretching band intensity. The matrix gases, argon and nitrogen (VEV, GDR) (or nitrogen obtained from liquid N_2), were purified by distillation in a vacuum system by a repeating cooling–warming cycle, using a liquid N_2 trap.

Infrared spectra of the matrices were recorded with a Perkin-Elmer 580B spectrophotometer operated in the integrated scan mode at a resolution of 1 cm^{-1}. No detectable absorption was observed in the CO_2 and H_2O regions, which might have originated if any leaks occurred in the vacuum system.

A continuous-flow liquid helium cryostat was employed. The solid sample was evaporated at the required temperature from a small electric furnace located near the cold window. The matrix gas was introduced simultaneously through a separate inlet, at a flow rate of several millimole/hour, initiated prior to turning on the heater and continued until the heater had returned to room temperature. Temperature was measured with a gold–iron-doped chromel thermocouple. The matrix gas was passed through a coil in the liquid-N_2-cooled jacket of the cryostat before deposition. The gas mixture was condensed on a CsI window maintained at the requisite low temperature (usually 10 K) by control of the helium flow in the cryostat. The concentration of the compound in the matrix was varied by regulating the temperature of the furnace during deposition. The time required to deposit sufficient sample for spectroscopic examination varied from one to several hours; the amount of sample deposited was monitored and controlled by following the absorbance of the strongest band in the carbonyl region. At the end of the matrix experiment, the sample contents remaining in the furnace were checked for possible thermal decomposition by UV spectroscopy and, occasionally, by chromatography. No indication of decomposition was found.

Matrix Effects. For better understanding of the spectra of matrix isolated species it is important to discuss briefly first the so-called "matrix effects" on the spectra. The assumption is usually made that the energy levels of trapped species are only slightly perturbed from their values in the gas phase. In fact, there must be some perturbation since small spectral band shifts are observed on going from the gas phase to argon and then to nitrogen matrices, reflecting local interactions between trapped molecules and the matrix. The trapped species, particularly larger molecules which replace more than one matrix atom, may find themselves in different local environments, with microcrystalline regions, having more or less different structures. This may result in a splitting of the band into distinct "site" components, appearing as shoulders on the main band, or just in broadening of the band if the splitting is small. It is frequently possible to obtain just one narrow band as a result of annealing the matrix. However, sometimes it is difficult to distinguish by annealing experiments between splitting produced by different transitions and by different trapping sites, particularly when annealing causes appearance of the bands due to self-association.

Additional problems are posed by the presence of traces of impurities, such as nitrogen, in the noble gas matrix.[12] The effect of impurities depends on the concentration ratio of matrix to trapped species, on the particular type of site, on the effective size of the cage, and on the energy of the interaction between the trapped molecule and the matrix. Larger trapped species, such as uracils, require a larger cage, and, hence, there is a higher probability of having an impurity molecule in the neighborhood. Examples and further discussion of such effects for 1-methyluracil in argon, xenon, and nitrogen matrices are given in ref 10.

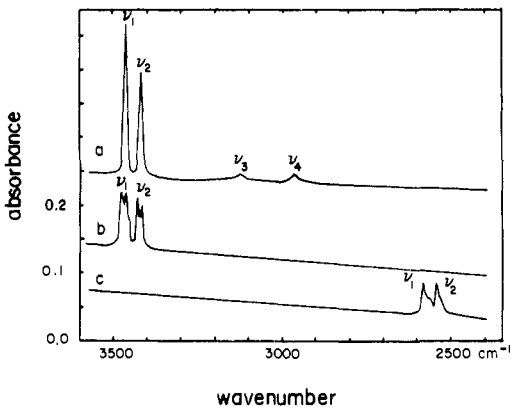

Figure 1. The infrared spectrum in the NH, ND, and CH stretching region of uracil (a) in nitrogen and (b) in argon matrices, and (c) of N_1,N_3-dideuteriouracil in an argon matrix. Assignment of the bands is the same as given in Tables I and II.

Results

The infrared spectra of uracil and N_1,N_3-dideuteriouracil in an argon matrix were studied from 350 to 4000 cm^{-1}. Spectra of uracil in nitrogen matrices were studied from 180 to 4000 cm^{-1}. These spectra are presented in Figures 1–4. Wavenumbers of the bands, maximum absorbances, and an assignment are summarized in Tables I and II. The observed spectra and the assignment are discussed below, organized separately for each spectral region.

Vibrational Assignment. In order to assign the frequencies of uracil based only on the infrared spectrum, we must draw heavily on previous assignments,[1,2,13-18] which have unfortunately been made using frequencies measured for solid uracil. Hence, we have supplemented this information by considering two recent quantum-mechanical calculations of frequencies of normal modes for the isolated molecule. The more extended calculation was made by Nishimura, Tsuboi, Kato, and Morokuma using an STO-3G basis set to predict frequencies.[16] The second, by Harsanyi and Csaszar,[18] used a CNDO/2 calculation scaled to fit frequencies from vapor data to preduct frequencies and intensities.

Although neither calculation, at this level, is expected to provide accurate predictions, both can be helpful in reaching a reliable assignment. The ab initio vibrational frequencies calculated by the STO-3G basis set[16] are expected to be more reliable than those from the scaled CNDO/2 calculations.[18] However, the STO-3G calculation predicts frequencies that are too high, and they must also be scaled by the usual approximate factor of 0.90 in order to bring them closer to agreement with 4-31G calculations for other molecules[16] or with the experimental spectrum (our data). Table I compares the experimental results with the STO-3G predicted frequencies, scaled by a constant factor of 0.90.

An assignment of frequencies based on the ab initio quantum-mechanical results would be more reliable if the relative intensities are also predicted. These predictions were not made with the STO-3G calculation[16] but have been given for the CNDO/2 calculations.[18] We have considered these predictions in making our assignment in Table I, but it is obvious that the intensity predictions are not quantitatively correct, even for relative intensities. For example, the intensities predicted for the CH stretching modes are an order of magnitude higher than for the

(9) M. Szczesniak, M. J. Nowak, K. Szczepaniak, and W. B. Person, to be submitted for publication (uracil concentrated in Ar and the pure solid).
(10) M. J. Nowak, M. Szczesniak, K. Szczepaniak, W. B. Person, and D. Shugar, to be submitted for publication (1-methyluracil in Ar, Xe, and N_2 matrices).
(11) Result for 3-methyluracil, 1,3-dimethyluracil, 2(4)-thiouracil, and 2,4-dithiouracil, cytosine, 9-methyladenine, and 9-methyguanine, in preparation for publication from our laboratory.
(12) (a) D. Maillard, A. Schriver, P. J. Perchard, C. Girardet, and D. Robert, *J. Chem. Phys.*, **67**, 3917 (1977); (b) R. Gunde, P. Felder, and H. Günthard, *Chem. Phys.*, **64**, 313 (1982).
(13) M. Tsuboi, S. Takahashi, and L. Harada in "Physiocochemical Properties of Nucleic Acids", Vol. 2, J. Duchesne, Ed., Academic Press, London, 1973.
(14) Y. Nishimura, A. Y. Hirakawa and M. Tsuboi in "Advances in Infrared and Raman Spectroscopy", Vol. 5, R. T. H. Clark and R. E. Hester, Eds., Heyden, London, 1978.
(15) Y. Nishimura, H. Haruyama, K. Nomura, A. Y. Hirakawa, and M. Tsuboi, *Bull. Chem. Soc. Jpn.*, **52**, 1340 (1979).
(16) Y. Nishimura, M. Tsuboi, S. Kato, and K. Morokuma, *J. Am. Chem. Soc.*, **103**, 1354 (1981).
(17) M. Shibata, T. J. Zielinski, and R. Rein, *Int. J. Quantum Chem.*, **18**, 323 (1980).
(18) L. Harsanyi and P. Csaszar, *Acta Chim. Acad. Sci. Hung.*, **113**, 257 (1983).

NH stretching modes, in direct contradiction with the experimentally observed relative intensities. Nevertheless, these predicted relative intensities have been included in Table I and we have considered them in the assignment discussed in more detail below.

4000–2000-cm^{-1} Region. This spectral region is shown in Figure 1a where we see that the only significant absorption for uracil in a nitrogen matrix is found in the NH stretching region at 3470 and 3423 cm^{-1}. The higher frequency is close to the N_1H stretching mode observed at 3462 cm^{-1} in an argon matrix spectrum of 3-methyluracil.[11] Similarly, the lower frequency is close to that observed at 3415 cm^{-1} for the N_3H stretching mode of 1-methyluracil in a nitrogen matrix.[10] Hence, we assign the 3470-cm^{-1} band to the N_1H stretching mode and the 3423-cm^{-1} mode to the N_3H stretch in uracil.

This straightforward assignment is further supported by our CNDO/2 calculations of the intensity of the N_1H mode relative to that of the N_3H mode.[19] This prediction is that the ratio of intensities is expected to be 1.3 for N_1H/N_3H in uracil and also 1.3 for the intensity ratio of the N_1H stretch in 3-methyluracil to that of the N_3H stretch in 1-methyluracil. This predicted value is very close to the intensity ratio of 1.4 observed for uracil in the matrix, and also the value of 1.3 for the vapor.[3] We do not understand why this ratio was predicted in the CNDO/2 calculation by Harsanyi and Csaszar[18] to be 3 rather 1.3, as quoted in Table I. The agreement for the NH stretching modes in Table I between the observed frequencies and those calculated by the STO-3G basis set strongly supports the value of 0.90 chosen for the scaling factor. On close examination we note that the STO-3G predicted wavenumber difference between the N_1H and N_3H stretching modes is only 25 cm^{-1} [16] (and only 22 cm^{-1} from the CNDO/2 calculation[18]), compared with 47 cm^{-1} observed, indicating that the calculations are still not absolutely correct.

Figure 1b shows this region of the spectrum of uracil in an argon matrix, and the wavenumbers, absorbances, and assignment are summarized in Table I. In this spectrum both N_1H and N_3H stretching modes split into doublets at 3482, 3467 cm^{-1} and 3433, 3422 cm^{-1}. This splitting might be due to a matrix site effect or to the effect on the uracil spectrum from nitrogen impurities preexisting in the argon. We prefer the latter interpretation because the lower frequency component of each doublet is close to, or equal to, the frequency of the corresponding band in the nitrogen matrix.

It is worthwhile to note that, for uracil vapor, two overlapped absorption bands in the NH stretching region are found at 3486 and 3445 cm^{-1}.[20] These frequencies are close to the matrix frequencies, indicating that the main species responsible for absorption in the matrix spectra are monomers. The slightly lower frequencies observed in argon and nitrogen matrix, compared with those in vapor [$(\nu_v - \nu_{Ar})_{N_1H}$ = 4 cm^{-1}, $(\nu_V - \nu_{Ar})_{N_3H}$ = 12 cm^{-1}; $(\nu_v - \nu_{N_2})_{N_1H}$ = 16 cm^{-1}, $(\nu_v - \nu_{N_2})_{N_3H}$ = 23 cm^{-1}], reflect the effect of the weak interactions of the N_1H and N_3H groups of the uracil molecule with the matrices. Note that shift in the N_3H mode is greater. No strong absorption between 3400 and 2800 cm^{-1} which could be assigned to the hydrogen-bonded self-associated molecules was found for uracil in the dilute matrices discussed here. Such absorption does appear in the spectra observed after annealing the matrix, when diffusion of molecules takes place to form dimers and higher aggregates. This subject is discussed elsewhere.[9]

Figure 1c shows the spectrum in the region for N_1,N_3-dideuteriouracil isolated in a dilute argon matrix. There is no trace of N_1H and N_3H absorptions indicating that deuteration is nearly 100% complete. Two bands are recorded at 2587 and 2549 cm^{-1}, both with shoulders on the lower frequency side. These bands are assigned as the N_1D and N_3D stretching modes, respectively. The ratio of frequencies is $\nu_s(N_1H)/\nu_s(N_1D) = \nu_s(N_3H)/\nu_s(N_3D)$ = 1.35, thus supporting the assignment. The lower frequency shoulders are probably due to the matrix site effects or to nitrogen impurities. No absorption was observed in the region below 2500 cm^{-1} for a dilute matrix, indicating that no hydrogen-bonded species are present.

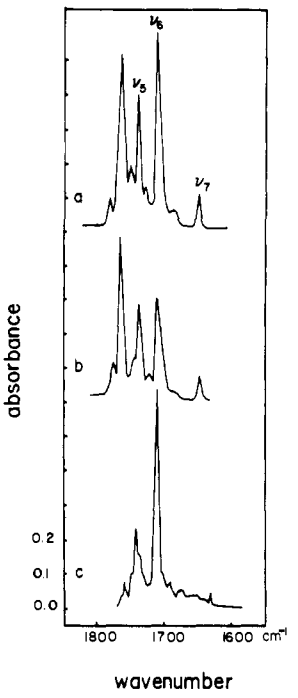

Figure 2. The infrared spectrum in the C=O and C=C stretching region of uracil (a) in an argon matrix. Assignment of the bands is the same as given in Tables I and II. Owing to the complication of this region by the Fermi resonance, it is difficult to show the correspondence of the bands of uracil and N_1,N_3-dideuteriouracil.

Studies in the NH (ND) stretching region provide important information on the tautomerism of uracil molecules isolated in a matrix. The appearance in the spectrum of only the N_1H and N_3H stretching modes with complete absence of any other absorption above 3500 cm^{-1} corresponding to the OH stretching vibration strongly suggests the uracil in argon and in nitrogen matrices is in the diketo tautomeric form; the ratio of other tautomeric forms (keto–enol and dienol (see ref 3)), if present at all, is less than 10^{-2} to 10^{-3}, as limited by the detectivity in infrared absorption. This conclusion is the same as that reached concerning tautomerism of uracil in the vapor phase.[3]

Two bands are expected in the CH stretching region of uracil, due to the C_5H and C_6H stretching modes. On close examination of the 3000–3100-cm^{-1} region of the matrix spectra shown in Figure 1, we see that two very weak peaks are observed near 3130 and 2970 cm^{-1}. These may be the C_5H and C_6H ν_3 and ν_4 fundamentals corresponding to the scaled predicted[16] bands at 3068 and 3031 cm^{-1} (or at 3112 and 3067 cm^{-1} according to ref 18), and we have made that assignment in Table I. The corresponding bands in the N_1,N_3-dideuterated uracil are too weak to be observed. The intensities of both CH stretching modes are certainly much lower than those of NH stretching modes in drastic contrast to the intensity predictions given in ref 18.

No absorption bands were observed in the region from 2400 to 1800 cm^{-1}, so this region is not shown in Figure 1.

1800–1600-cm^{-1} Region. In this region we expect to find three more fundamental modes of vibration for uracil, namely, the C_2=O and C_4=O carbonyl stretching modes and the C_5=C_6 ring stretching mode. Certainly we may expect to find them strongly mixed with each other and with other group frequency motions including the C–N ring stretches and the two N_1H and N_3H in plane bending modes. Nishimura et al.[16] have given potential energy distributions (PEDs) indicating strong mixing of the coordinates in this region, in contrast with the characteristic group-frequency behavior in the 3000–4000-cm^{-1} region.

Examining the spectrum of uracil in the nitrogen matrix shown in Figure 2a, we see that the absorption pattern in this region is much more complicated than expected. Three strong bands are

(19) T. Nasierowski, M. S. Thesis, University of Warsaw, 1978.

(20) We have reinvestigated the vapor spectrum of uracil using a longer cell (10 cm) with the Perkin-Elmer 580B spectrometer and measured the N_1H and N_3H stretching frequencies at 3486 and 3445 cm^{-1}. The previous values, reported in ref 3, were 3483 and 3437 cm^{-1}, respectively.

Table I. Observed Frequencies and Absorbances of Uracil in a Nitrogen and Argon Matrix Compared with the Predicted Frequencies[16,18] and Absorbances[18]

		calculated			experimental				
			scaled CNDO/2[d]		previous[e]	this work			
						in nitrogen[f]		in argon	
mode	assignment[a,b]	scaled[c] STO-3G, cm^{-1}	frequency, cm^{-1}	rel absorbance	frequency, cm^{-1}	frequency, cm^{-1}	rel absorbance[g]	frequency, cm^{-1}	rel absorbance[g]
				In-Plane Vibrations					
ν_1	N_1H str [99]	3478	3460	3	3395	3470	139	3482[i]	125
								3467[i]	100
ν_2	N_3H str [99]	3453	3438	1	3395	3423	100	3433[i]	100
								3422[i]	75
ν_3	C_5H str [95]	3068	3112	10	3100	3130	4	3130	15
ν_4	C_6H str [95]	3031	3067	64	3080	2970	8	2970	15
						1779	111	1774	125
ν_5	C_2=O str [53]	1775	1765	1788	1716	1766	sh	1762	672
						1761	600		
						1756	367	1758	312
						1748	100		
ν_6	C_4=O str [56]	1748	1739	681	1675	1736	489	1733	350
						1727	133		
						1724	122	1720	62
						1707	sh	1707	375
						1704	711	1699	163
ν_7	C_5=C_6 str [57]	1664	1614	41	1611	1645	67	1644	100
						1598 imp	11		
$2\nu_{24}$	overtone					1526	17	1525	25
ν_8	ring str [50] N_1H bend [26]	1483	1503	91	1508	1477	83	1473	125
ν_9	ring str [55] N_3H bend [32]	1397	1446	20	1453	1463 or 1388	15 17	1461 or 1389	25 38
ν_{10}	N_3H bend [20] + CH bend [35]	1379	1392	211	1417	1405	163	1401	138
ν_{11}	ring str [39] N_1H bend [30]	1372	1340	7	1390	1388 or 1369	17 17	1389[i] 1283[i] or 1366	38 25 13
$\nu_{24} + \nu_{27}$						1354 imp	17	1361 imp 1314	13 10
ν_{12}	ring str [63]	1247	1225	5	1238	1220	6	1219	13
ν_{13}	CH_{ooph} bend [64]	1171	1104	39	1217	1192	150	1186	413
ν_{14}	ring str [55]	1064	1040	21	1099	1070	11	1076	50
ν_{15}	ring def [75]	978	996	13	1003	977	11	963	13
ν_{16}	ring str [61]	932	923	29	993	965	17	958	25
ν_{17}	CC str ring def CN str[d]		773	26	781	724	17	719	14
	ring breathing [67]	740							
ν_{18}	ring def ooph		597	25				557 or	25
	ring def [57]	551			581	557	11	551	25
ν_{19}	ring def ooph[d]		528	27					
	C=O i ph bend [60]	532	525	39	565	538	17	537	25
ν_{20}	ring def [67]	502	519	402	550	518	61	516	125
ν_{21}	C=O bend [69]	374	365	26		401[i] 394[i]	28 44	393	25
				Out-of-Plane Vibrations					
ν_{22}	CH bend		921	71	822	846	6		
ν_{23}	C_4=O bend		813	190		811	83	806	175
	CH bend					808	72		
ν_{24}	C=O bend		754	220	782	762	100	769	125
ν_{25}	CH bend		669	14	760	677	28	685	14
								682	13
ν_{26}	NH bend		519	402	851	685	50	664	100
ν_{27}	NH bend		469	164	830	592	33	585 or 557	13 or 25
ν_{28}	torsion		340	137	435				
ν_{29}	torsion		151	11					
ν_{30}	torsion		88	3					

[a] Based on the normal coordinate calculation described by Nishimura et al.[16] Their potential energy distribution (PED) is given in brackets. The out-of-plane modes (ν_{22}–ν_{30}) are assigned based on the CNDO/2 calculation.[18] [b] Abbreviations: str, stretching; bend, bending; def, deformation; i ph, in phase; ooph, out of phase. [c] The wavenumbers calculated with the STO-3G in ref 16 have been scaled by multiplying them all by 0.9 to give the numbers listed here. [d] The wavenumbers calculated with the CNDO/2 method in ref 18 were scaled as described there to give the predicted values listed here. [e] These values are a summary of experimental wavenumbers that were assigned previously and listed by Nishimura et al.[16] and by Susi and Ard.[1] These values are from observed spectra for uracil in the solid or in solution in polar solvents and the differences between the values given here and those in "this work" are often primarily due to intermolecular interactions rather than to reassignment to different modes. [f] All the bands observed for uracil isolated in an N_2 matrix are listed here. [g] The maximum absorbance for each band relative to that for ν_2 [abs(ν_2) = 100] is listed here. [h] These bands are due to the two fundamental modes expected here in Fermi resonance with one or more combination bands (see text). [i] Matrix splitting.

Table II. Observed Frequencies and Absorbances of N_1,N_3-Dideuteriouracil in an Argon Matrix Compared with the Predicted Frequencies[16]

mode	assignment[a]	calculated: scaled[b] STO-3G, cm^{-1}	experimental: previous[c] frequency, cm^{-1}	experimental: this work frequency, cm^{-1}	experimental: this work rel absorbance[d]
		In-Plane Vibrations			
ν_1	N_1D str		2330	2587	100
ν_2	N_3D str		2277	2549	100
ν_3	C_5H str		3087		
ν_4	C_6H str		3087		
ν_5	C_2=O str	1757	1704	1767	100
				1762	200
				1750	250
ν_6	C_4=O str	1743	1650	1744	675
				1739	400
				1713	1625
				1703	250
				1684	175
				1675	80
				1656	60
ν_7	C_5=C_6 str	1653	1609	1634	100
$2\nu_{24}$	overtone			1512	50
ν_8	ring str	1463	1471	1440	500
				1432[e]	200
				1450	125
ν_9	ring str N_3D bend	1115		1113	50
ν_{10}	CH bend N_3D bend	1382	1340	1380	226
ν_{11}	ring str N_1D bend	~900		915	30
ν_{12}	ring str	1328	1165	1255	50
ν_{13}	CH bend	1292	1236	1318	225
ν_{14}	ring str	1148	981	?	?
ν_{15}	ring def	972	965	970	20
ν_{16}	ring str N_3D bend	810	883	777	50
ν_{17}	ring breathing	738	778	724	20
ν_{18}	ring def	545	560	543	20
ν_{19}	C=O bend	527	542	524	20
ν_{20}	ring def	491		508	100
ν_{21}	C=O bend	371		388	100
		Out-of-Plane Vibrations			
ν_{22}	CH bend		822	829	20
ν_{23}	C=O bend CH bend		788	803	250
ν_{24}	CH bend or C=O bend		762	758	200
ν_{25}	C=O bend or CH bend			768	30
ν_{26}	ND bend		621		
ν_{27}	ND bend		584		
ν_{28}	torsion		431		
ν_{29}	torsion		431		
ν_{30}	torsion		431		

[a] Based on the normal coordinate calculation described by Nishimura et al.[16] Abbreviations are in Table I. [b] Scaled STO-3G frequencies of N_1,N_3-dideuteriouracil were estimated from Figure 2 in ref 16 and multiplied by factor 0.9. [c] Frequency from ref 1 for solid N_1,N_3-dideuteriouracil. [d] The maximum absorbance for each band relative to that for ν_2 (abs(ν_2) = 100 is listed here. [e] Matrix splitting.

observed in the carbonyl region at 1761, 1736, and 1704 cm^{-1}, complicated by several weaker features, with a sharp medium-strength line at 1645 cm^{-1}.

In the argon matrix the spectrum is similar (see Figure 2b), but the relative intensity pattern is slightly different. In the spectrum of N_1,N_3-dideuteriouracil in argon shown in Figure 2c, a different spectral pattern is observed in the carbonyl region, with a strong band at 1713 cm^{-1} and a medium band at 1744 cm^{-1}, together with a relatively weak band at 1634 cm^{-1} and several other weak bands or shoulders with frequencies given in Table II.

It is worthwhile to note that for uracil vapor[3] strong and broad absorption is observed in the region 1800–1600 cm^{-1} with a maximum at 1765 cm^{-1} and a separate weak feature at 1640 cm^{-1}. The rotational broadening of this band does not allow us to distinguish the number of separate vibrational components that contribute to this broad absorption.

From these observations it seems clear that the lower frequency mode (1645 cm^{-1} in the nitrogen matrix) should be assigned to the C_5=C_6 "ring stretching mode" predicted by the scaled STO-3G calculation[16] to be at 1664 cm^{-1} with 57% PED from the C_5=C_6 stretch. Apparently the two carbonyl stretching modes in the N_1,N_3-dideuteriouracil interact with some other modes in the uracil molecule to produce the pattern of the remaining three dominant bands observed in the nitrogen matrix.

Examples of extra peaks occurring in the carbonyl region of the spectrum have been seen before.[21-23] The most likely explanation for effects such as those observed here in Figure 2 is that Fermi resonance occurs between the strong carbonyl fundamentals and overtone or combination bands from the lower frequency modes. Some of the shoulders could also be due to the matrix site effects, but the absence of dimer and polymer bands in the NH stretching region reduces the likelihood that such intermolecular interactions are responsible for the complexity of this region.

At least five combination bands will have the same symmetry as the carbonyl stretches and occur in that spectral region: $\nu_{10} + \nu_{21}$ (1799 cm^{-1}), $\nu_{13} + \nu_{18}$ (1749 cm^{-1}), $\nu_{13} + \nu_{19}$ (1730 cm^{-1}), $\nu_{13} + \nu_{20}$ (1710 cm^{-1}), and $\nu_{16} + \nu_{17}$ (1689 cm^{-1}). All these wavenumbers are calculated from data in the nitrogen matrix, assuming no anharmonicity. These combination frequencies would be lower for more realistic anharmonic vibrations. If the Fermi resonance matrix elements for the interaction of even one of these combinations with both carbonyl fundamentals is large enough, a complicated triple Fermi resonance can be expected among the three modes.[24] This resonance will transfer intensity among the three modes in a complicated pattern which will change drastically in different environments as the frequency of any one of the normal modes involved is shifted. Such behavior seems entirely consistent with the experimental patterns observed in Figure 2 (see also our paper on 1-methyluracil in different matrices, ref 10). We note that both the high-frequency combination modes listed above shift out of range for Fermi resonance in N_1,N_3-dideuteriouracil ($\nu_{13} + \nu_{18}$ to 1861 cm^{-1} and $\nu_{13} + \nu_{20}$ to 1826 cm^{-1}) and so the Fermi resonance might be less important in that molecule. A more detailed analysis of Fermi resonance in the carbonyl stretching region for uracil, 1(3)-methyl- and 1,3-dimethyluracil, and 2-(4)-thiouracils will be given elsewhere.[25]

On the basis of the studies presented here it is not possible to decide which of the bands is due to the C_2=O stretch and which to the C_4=O stretch. The arguments based on frequency shifts for ^{18}O-substituted uracil in water[26] suggest that the highest frequency carbonyl mode is the C_2=O mode, as does the order of the calculated frequencies given by Nishimura et al.[16] The intensities predicted in ref 18 suggest that the higher frequency C_2=O stretch should be the most intense, in agreement with the observed spectrum of uracil in argon, but in contradiction with the observed spectrum of uracil in the nitrogen matrix. We have kept for now the usual assignment in Table I that the C_2=O stretching mode is at higher wavenumber than the C_4=O stretch.

(21) D. Shugar and K. Szczepaniak, *Int. J. Quantum Chem.*, **20**, 573 (1981).
(22) M. C. Delvaux-de Wilde and Th. Zeegers-Huyskens, *Spectrosc. Lett.*, **12**, 7 (1979).
(23) ML. S. Bellamy, "Advances in Infrared Group Frequencies", Chapman and Hall, London, 1975.
(24) M. P. Lisitsa, N. E. Talko, and A. M. Yeremko, *Opt. Spectrosc. (USSR)*, **28**, 235 (1970).
(25) K. Szczepaniak and W. B. Person, to be submitted for publication.
(26) H. T. Milles, T. P. Lewis, E. D. Becker, and J. Frazier, *J. Biol. Chem.*, **243**, 1115 (1973).

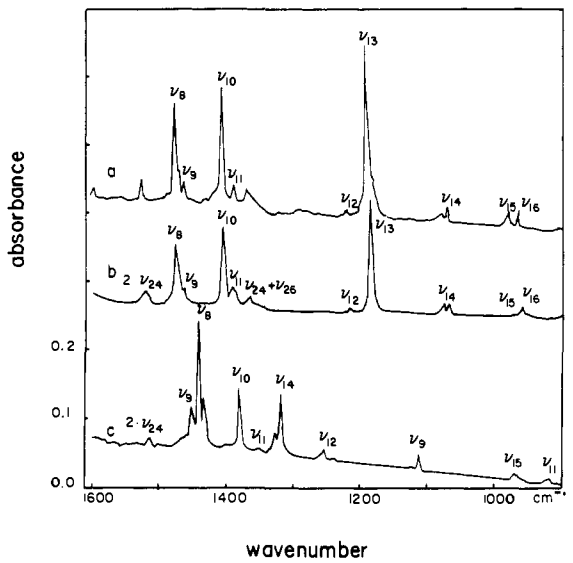

Figure 3. The infrared spectrum in the ring stretching and bending and in NH, CH bending region of uracil (a) in nitrogen and (b) in argon matrices, and (c) for N_1,N_3-dideuteriouracil in an argon matrix. Assignment of the bands is the same as given in Tables I and II.

1600–400-cm^{-1} Region. The spectra in this region of matrix-isolated uracil and N_1,N_3-dideuteriouracil are given in Figures 3 and 4. This region contains absorption from the remaining 14 in-plane vibrations of both molecules. There are several regions of rather strong absorption in Ar and in N_2 matrices, clearly corresponding to absorption by fundamental modes. In addition there are a number of weaker absorption bands. Most of them also are to be assigned to fundamental modes. The problem now is to decide which of these absorptions correspond to which fundamental mode. In the absence of matrix infrared spectra of all possible deuterated molecules (e.g., C_5,C_6-dideuterated uracil and perdeuterated uracil) and also of the Raman spectra of matrix isolated uracil and of deuterated uracils, it is difficult to make any very definite assignment. We have chosen, under these circumstances, to continue our assignment using the scaled STO-3G calculations from Nishimura et al.,[16] as well as the CNDO/2 calculations from Csaszar and Harsanyi[18] and previous assignments based on infrared and Raman spectra of solids from Susi and Ard.[1]

The resulting assignment is summarized in Table I. We use the nomenclature and description of the vibrations given by the PEDs of Nishimura et al.[16] First of all we try to correlate the most intense bands of uracil and its N_1,N_3-dideuterated analogue. Examining the spectra in Figure 3 we assigned the strong band at 1477 cm^{-1} as ν_8 related mainly to ring stretching modes (50%) with some contribution from $\delta(N_1H)$ (26%). We expect that this band shifts to 1440 cm^{-1}, where a strong band appears, in the spectrum of N_1,N_3-dideuterated uracil. The assigned frequency of ν_8 and the observed shift upon N_1,N_3-dideuteration both agree well with STO-3G and CNDO/2 predictions as far as scaled frequencies and relative intensities are concerned and also with the previous assignment.[1] The next strong band in the spectrum shown in Figure 3 is the one at 1405 cm^{-1} in the N_2 matrix and at 1401 cm^{-1} in the Ar matrix. We assigned it as ν_{10}, since its frequency is close to the frequency predicted for that mode by STO-3G[16] and CNDO/2[18] calculations, and also its relatively high intensity is in agreement with CNDO/2 predictions.[18] It has significant contribution from δ(CH) (35%) and $\delta(N_3H)$ (20%). The band assigned as ν_{10} shifts to 1380 cm^{-1} in N_1,N_3-dideuterated uracil in agreement with its STO-3G predicted frequency and remains one of the strong bands in the spectrum of the deuterated homologue. The frequency of absorption assigned here as ν_{10} is also close to the frequency of ν_{10} assigned by Susi and Ard.[1]

The third strong absorption found in the spectrum shown in Figure 3 at 1192 cm^{-1} in N_2, and 1186 cm^{-1} in Ar, was assigned as ν_{13}. It is expected to have 16% contribution from ring-stretching vibrations, 10% contribution from $\delta(N_1H)$, and 64% contribution from δ(CH). As the corresponding band in the spectrum of N_1,N_3-dideuterated homologue, we chose the third strong band in its spectrum in Figure 3c at 1318 cm^{-1}. This band is significantly shifted toward higher frequencies with respect to the corresponding band of uracil, and such a shift toward higher frequency upon N_1,N_3-dideuteration is predicted from the STO-3G calculations.[16] In fact, this large shift to higher frequency upon deuteration and high intensity is the most important argument in favor of the chosen assignment of ν_{13} for uracil and N_1,N_3-dideuteriouracil. It should be noted that CNDO/2 calculations of relative intensities predict that the ν_{13} vibration will be a much weaker vibration than ν_8 and ν_{10} (see Table I).

Now, we have to assign to other fundamental modes several weak absorptions found in Figure 3 for uracil and N_1,N_3-dideuteriouracil. As before, we have been guided by the STO-3G[16] and CNDO/2[18] calculations and by previous assignments. As ν_9 we assigned the weak absorption at 1463 (or 1388) cm^{-1} in N_2 and at 1461 (or 1389) cm^{-1} in Ar. According to the STO-3G predictions[16] the scaled frequency of this band is 1397 cm^{-1}, and the main contribution to this mode is from ring stretching (50%) and $\delta(N_3H)$ (32%) motions. The CNDO/2 calculation predicts ν_9 at 1446 cm^{-1} and according to previous work ν_9 is located at 1453 cm^{-1} in the solid. According to ref 16, N_1,N_3-dideuteration causes splitting of this mode into one which is almost not shifted, and another which is shifted strongly to lower frequencies. However, only one vibration corresponding to ν_9 can occur in the deuterated compound, so the apparent "splitting" must indicate an uncertainty about whether this mode is expected to shift on deuteration. If it does not, the absorption in the deuterated molecule at 1450 cm^{-1} may be ν_9; if it should shift, the weak absorption at 1113 cm^{-1} may be ν_9 (Figure 3c).

The ν_{11} mode according to the STO-3G scaled prediction, should be located near 1372 cm^{-1} and should have 39% contribution from ring stretching and 30% contribution from $\delta(N_1H)$. According to the CNDO/2 prediction, it is expected at 1340 cm^{-1}. Susi and Ard[1] assigned ν_{11} at 1390 cm^{-1}. The absorption at 1388 cm^{-1} in N_2 is assigned as ν_{11}. Deuteration is expected[16] to shift ν_{11} to about 900 cm^{-1}. Taking this into account we assigned as ν_{11} of N_1,N_3-dideuterated uracil a weak band at 915 cm^{-1} (Figure 3c).

The ν_{12} mode is expected[16] at 1247 cm^{-1}. It should have a 63% contribution from ring stretching vibrations and 21% contribution from $\nu(N_3H)$. The CNDO/2 calculation[18] predicts ν_{12} at 1225 cm^{-1}, and in ref 1, ν_{12} was assigned at 1238 cm^{-1}. According to ref 16 N_1,N_3-dideuteration should shift ν_{12} to higher frequencies. These predictions can be fulfilled if we assign as ν_{12} of uracil the weak absorption at 1220 cm^{-1} in N_2 (and at 1219 cm^{-1} in Ar) and the weak band at 1255 cm^{-1} as ν_{12} of N_1,N_3-dideuteriouracil.

The ν_{14} mode is expected at 1064 cm^{-1} according to the STO-3G prediction[16] with 22% contribution from δ(CH), about 10% from $\delta(N_1H)$, and about 55% from ring stretching vibrations. The CNDO/2 prediction of ν_{14} is at 1104 cm^{-1}.[18] According to Nishimura et al.,[16] ν_{14} is expected to shift slightly downward upon N_1,N_3-dideuteration. As ν_{14} of uracil we have assigned a weak band at 1070 cm^{-1} in N_2 (1076 cm^{-1} in Ar) (Figure 3a,b). In N_1,N_3-dideuteriouracil we believe that ν_{14} is probably too weak to be observed. Susi and Ard[1] assigned the absorption at 1236 cm^{-1} to ν_{14}.

We assigned ν_{15} of uracil to the weak band at 977 cm^{-1} in N_2 (hardly visible at 963 cm^{-1} in Ar) which shifts to near 970 cm^{-1} in the spectrum of N_1,N_3-dideuterated uracil in Ar. The previous assignment of ν_{15}[1] was at 1003 cm^{-1}, and the scaled CNDO/2 prediction for ν_{15} was at 996 cm^{-1}.[18] The STO-3G calculation predicts ν_{15} at 978 cm^{-1} and its shift upon N_1,N_3-dideuteration to about 972 cm^{-1}.[16] According to the latter calculation the main contribution to ν_{15} comes from the ring deformation vibration (75%).

As ν_{16} of uracil we assign the weak absorption band at 965 cm^{-1} in N_2 (958 cm^{-1} in Ar). According to the STO-3G calculation ν_{16} is expected at 932 cm^{-1} and the most important contributions to this vibration are from ring stretching (61%) and $\delta(N_3H)$ (10%) vibrations. The predicted[16] shift downward upon deuteration is

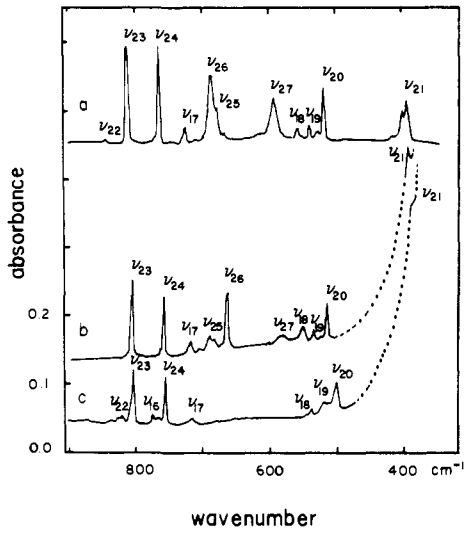

Figure 4. The infrared spectrum in the ring breathing and deformation, C=O and ND bending, and out-of-plane bending region of uracil (a) in nitrogen and (b) in argon matrices, and (c) for N_1,N_3-dideuteriouracil in an argon matrix. The assignment for the bands of uracil and N_1,N_3-dideuteriouracil is the same as given in Tables I and II. Spectra b and c were studied using a KBr cold window. The increasing absorption (broken line) below 500 cm^{-1} is due to the increasing absorption from the KBr window. Spectrum a was studied with a CsI cold window.

about 150 cm^{-1}. Taking this into account we assigned tentatively the weak absorption at 777 cm^{-1} (Figure 4c) as ν_{16} of the N_1,N_3-dideuterated compound. The previous assignment of ν_{16} was at 993 cm^{-1} for solid uracil and 883 cm^{-1} for solid N_1,N_3-dideuteriouracil.[1] The scaled CNDO/2 prediction[18] for ν_{16} of uracil was 923 cm^{-1}.

The ν_{17} mode of uracil was assigned to the weak absorption at 724 cm^{-1} in N_2 (719 cm^{-1} in Ar) (Figure 4a,b) and that of N_1,N_3-dideuterated uracil to the weak absorption at 724 cm^{-1} (Figure 4c). This assignment was chosen because the scaled STO-3G predicted wavenumber for ν_{17} is 740 cm^{-1} with little change upon N_1,N_3-dideuteration (the main contribution is ring breathing (67%)) and because the scaled CNDO/2 prediction for ν_{17} is 773 cm^{-1}, also in fairly good agreement with our assigned value.

Between 600 and 500 cm^{-1}, both STO-3G[16] and CNDO/2[18] calculations predict that ν_{18}, ν_{19}, and ν_{20} modes will appear. We assigned as ν_{18}, ν_{19}, and ν_{20} respectively the absorption bands occurring for uracil at 557, 538, and 518 cm^{-1} in the N_2 matrix (557, 537, and 516 cm^{-1} in Ar). Such assignments for these bands agree reasonably well with the predicted frequencies (551, 532, and 505 cm^{-1} by STO-3G[16] and 548, 525, and 519 cm^{-1} by CNDO/2[18]. In agreement with the CNDO/2 predictions,[18] the strongest of all three bands in this range is ν_{20}. The predicted[16,18] contributions to ν_{18}, ν_{19} and ν_{20} come mostly from ring deformation and from C=O bending vibrations (see Table I and Figure 4).

Finally, as the last in-plane vibration, ν_{21}, we have assigned the medium strength absorption at 401 cm^{-1} in N_2 (split into a doublet, probably due to matrix splitting) and at 393 cm^{-1} in Ar. The scaled predicted frequency of ν_{21} is 374 cm^{-1} (STO-3G[16]) and 365 cm^{-1} (CNDO/2[18]). The main contribution to ν_{21} is expected[16] to come from the C=O bending (69%). No significant shift upon N_1,N_3-dideuteration is expected, and in agreement with this we assigned the weak band at 388 cm^{-1} (Figure 4c) as ν_{21} of N_1,N_3-dideuteriouracil.

The out-of-plane modes were not considered by Nishimura et al.[16] because of computational difficulties. Here we have been guided by the frequencies predicted by the CNDO/2 calculations in ref 18.

The out-of-plane CH bending mode ν_{22} γ(CH) is expected[18] to be at 921 cm^{-1}. As may be seen in Figure 3 no significant absorption is observed near this wavenumber for uracil either in nitrogen or in an argon matrix. Instead a very weak absorption is found at 846 cm^{-1}, which we have assigned as ν_{22}. This wavenumber is close to that assigned in ref 1 to ν_{22} for solid uracil. The very weak band at 822 cm^{-1} for N_1,N_3-dideuteriouracil is assigned as ν_{22}.

The strong absorption at 806 cm^{-1} for uracil in the argon matrix is assigned to ν_{23} ($\gamma_{C_4=O}$ + γ_{C-H}). In the nitrogen matrix this band splits into a doublet, probably due to matrix effects. This assignment agrees very well with the predicted value[18] of 813 cm^{-1}. Another strong band at 762 cm^{-1} for uracil in nitrogen and 769 cm^{-1} in argon was assigned as ν_{24} ($\gamma_{C_2=O}$), predicted[18] at 762 cm^{-1}.

Strong absorption bands assigned as ν_{23} and ν_{24} were also observed for N_1,N_3-dideuteriouracil in the argon matrix at 803 and 758 cm^{-1}. Our assignment of ν_{24} is the same as that given by Harsanyi and Csaszar[18] but differs from assignment by Susi and Ard[1] of this band to ν_{25} γ(CH). The principal distinction between these two assignments is the intensity prediction[18] that ν_{24} should be relatively strong.

We have tentatively assigned ν_{25} γ(CH) to the weak absorption at 677 cm^{-1} appearing as a shoulder on the strong sharp absorption at 685 cm^{-1} in the spectrum of the nitrogen matrix (Figure 4a) and as a weak broad band at 680 cm^{-1} in the argon matrix.

Two relatively strong bands are observed for uracil in the nitrogen matrix at 685 and 592 cm^{-1} (Figure 4a). In an argon matrix a strong sharp band at 664 cm^{-1} and weak and relatively broad bands at 585 or 551 cm^{-1} are observed (Figure 4b). These bands are absent from the spectrum of N_1,N_3-dideuteriouracil, strongly suggesting that they have γ(NH) character. Hence we have assigned the stronger band at 685 cm^{-1} in the nitrogen matrix and at 664 cm^{-1} in argon to ν_{26} and the band at 592 cm^{-1} in nitrogen and at 585 or 551 cm^{-1} in argon to ν_{27} γ(NH) with the other weak features at 682 cm^{-1} in argon (677 cm^{-1} in nitrogen) to the coupled ν_{25} γ(CH) vibration as stated above. The weak bands near 682 and 585 cm^{-1} in argon matrix could also be nitrogen induced ν_{26} and ν_{27} bands, respectively (see Figure 4).

We note in Table I that the predicted[18] value of ν_{25} (669 cm^{-1}) agrees very well with our assigned value, but the predicted values[18] for ν_{26} and ν_{27} (519 and 469 cm^{-1}) are much too low. As can be seen in Figure 4, we do not observe any bands below 550 cm^{-1} which have γ(NH) character.

If the γ(ND)/γ(NH) ratio were about 1.35, we expect the γ(ND) bands in N_1,N_3-dideuteriouracil to absorb around 500 and 437 cm^{-1}, but no significant absorption is observed in this region (Figure 4c). Probably the intensity of these absorption bands in the deuterated compound is too low, so that they are not observed.

The last three out-of-plane vibrations [(ν_{28} (torsion 1), ν_{29} (torsion 2), and ν_{30} (torsion 3)] are predicted[18] to be at 340, 151, and 88 cm^{-1}, respectively, below the region which could be studied in our experiment.

Conclusions

It is quite clear that the vibrational frequencies for the uracil molecule isolated in the matrix are different from those for the interacting molecule previously observed in the solid or in polar solutions. Tables I and II compare our observed frequencies, and our assignment, with the assignment of the experimental frequencies given by Nishimura et al.[16] and by Csaszar and Harsanyi.[18] We shall discuss in another paper the relationship between the spectra of uracil in different phases and try to understand better the reason for the differences between the spectrum of the molecule isolated in a matrix and that for the same molecule when it interacts with other molecules. Each kind of spectrum can have its own interest for biologically interesting molecules. Clearly, the matrix-isolated molecule is closer to the truly isolated molecule for which quantum-mechanical model calculations can be made. The agreement between our assignment and the scaled STO-3G predictions is phenomenal, as of course it should be since it is based on the latter. As further experimental data become available, this assignment can be tested more critically. If it fails, as can be expected for at least some of its details, the calculations can be refined further. Until then, the theoretically predicted frequencies have been extremely helpful in making this first assignment. We note in conclusion that accurately predicted intensities would be even more helpful in making an assignment of this kind. The ab

initio calculations of intensities of uracils are in progress at the University of Florida.[27] The preliminary results confirm the assignment given here.

Acknowledgment. We wish to express our thanks to Professor J. Kolodziejczak for his interest in this work and his help with the initiation of this investigation in the Institute of Physics of the Polish Academy of Sciences. We are grateful to Mr. A. Orlowski for his permanent instrumental and technical assistance. The writers wish to express their thanks to Dr. A. J. Barnes for his critical remarks and suggestions based on the yet unpublished matrix studies of uracils performed at the University of Salford. This investigation was supported by the Polish National Cancer Research Program (Project PR-6) and by Institute of Physics PAN Research Grant (Project C-1). In addition W.B.P. is grateful for partial financial support from NSF Research Grant No. CHE 81-01131.

(27) S. Chin, I. Scott-Lebron, K. Szczepaniak, and W. B. Person, to be submitted to *J. Am. Chem. Soc.*

Registry No. Uracil, 66-22-8; N_1,N_3-dideuteriouracil, 20666-60-8.

Ionized Oxycarbenes: $[COH]^+$, $[HCOH]^{+\cdot}$, $[C(OH)_2]^{+\cdot}$, $[HCO_2]^+$, and $[COOH]^+$, Their Generation, Identification, Heat of Formation, and Dissociation Characteristics

Peter C. Burgers, Alexander A. Mommers, and J. L. Holmes*

Contribution from the Chemistry Department, University of Ottawa, Ottawa, Ontario, Canada K1N 9B4. *Received March 2, 1983*

Abstract: The title ions have been generated by appropriate dissociative ionizations and identified by means of their collisional activation mass spectra. Their heats of formation have been measured via appearance energies, ΔH_f for $[COH]^+$, $[HCOH]^{+\cdot}$, $[C(OH)_2]^{+\cdot}$, and $[COOH]^+$ being 220, 238, 175, and 141 kcal mol^{-1}, respectively. The new ions do not readily isomerize to their better known counterparts $[HCO]^+$, $[H_2CO]^{+\cdot}$, $[HCOOH]^{+\cdot}$, there being large energy barriers thereto. For ionized formaldehyde and formic acid the barriers both lie at least 34 kcal mol^{-1} above $[HCOH]^{+\cdot}$ and $[C(OH)_2]^{+\cdot}$. Isotopic labeling experiments permitted the separation of two dissociation pathways for $[HCOH]^{+\cdot}$, one leading to $[HCO]^+$ and the other to $[COH]^+$. Measurement of metastable peak appearance energies showed that the reactions $[HCO]^+ + H\cdot \rightarrow [HCOH]^{+\cdot}$ and $[COOH]^+ + H\cdot \rightarrow [C(OH)_2]^{+\cdot}$ have critical energies of ca. 1 eV, whereas the reactions leading respectively to $[H_2CO]^{+\cdot}$ and $[HCOOH]^{+\cdot}$ have none.

Introduction

Laboratory observations[1,2] of the proposed interstellar species[3] $[COH]^+$ have recently been reported. The ion was generated by dissociative ionization of CD_3OH, and its collisional activation (CA) mass spectrum permitted its ready distinction from the isomeric ion $[HCO]^+$. These experiments were in part prompted by ab initio calculations[4] at a high level of theory, which predicted the heat of formation, $\Delta H_f[COH]^+$, to be 232 kcal mol^{-1} and a high barrier to its exothermic rearrangement to $[HCO]^+$. It should be noted that $[COH]^+$ had been proposed to be generated from CD_3OH by Berkowitz[5] and Momigny et al.,[6] but unequivocal identification of the structure was lacking in these reports. The finding that $[COH]^+$ can readily be identified raised our interest in searching for the related small oxy cations of structure $[HCOH]^{+\cdot}$, $[C(OH)_2]^{+\cdot}$, and $[HCO_2]^+$. $[HCOH]^{+\cdot}$ was recently reported by Wesdemiotis and McLafferty,[7] but its thermochemistry was not determined.

In this paper we describe methods for the production of the above ions, their CA mass spectra, their ΔH_f values, and the magnitude of the energy barriers to their isomerization to $[HCO]^+$, $[H_2CO]^{+\cdot}$, $[HCOOH]^{+\cdot}$, and $[COOH]^+$, respectively. Where appropriate, results will be compared with ab initio calculations.

Table I. Partial Collisional Activation Mass Spectra[a] of $[CH_2O]^{+\cdot}$ Ions

precursor	fragment ion m/z					
	12	13	14	16	17	18
H_2CO	18	23	43	10	5	1
CH_2CH_2CHOH	18	45	7	4	18	8
CH_3OH	17	46	9	4	17	7

[a] m/z 28 and 29 (unimolecular reaction) omitted. Intensities relative to $\Sigma = 100$, values ±1.

Results and Discussion

The Hydroxymethylidyne Cation $[COH]^+$. Ab initio calculations[4] have explored the potential energy surface for $[COH]^+$ and $[HCO]^+$ and found that the ground state of $[COH]^+$ lies 37.5 kcal mol^{-1} above $[HCO]^+$. The isomerisation barrier was calculated to be 36 kcal mol^{-1} above $[COH]^+$, appreciably below the threshold for the least endothermic reaction to $H^+ + CO$, a further 71 kcal mol^{-1}. These results therefore show that the isomers can interconvert below their dissociation energy. It has been observed[1,2] that the CA mass spectrum of m/z 29 from CD_3OH was different from the ion produced by simple bond cleavages, such as m/z 29 from CH_3CHO, which has the structure $[HCO]^+$. The spectra are shown in Figure 1 and the ion derived from CD_3OH was assigned the structure $[COH]^+$; the abundance of m/z 13 and 16 are clearly structure diagnostic. However, $[COH]^+$ is generated from CD_3OH together with a small amount of its isomer $[HCO]^+$.

(1) Illies, A. J.; Jarrold, M. F.; Bowers, M. T. *J. Chem. Phys.* **1982**, *77*, 5847.
(2) Burgers, P. C.; Holmes, J. L. *Chem. Phys. Lett.* **1983**, *97*, 236.
(3) Irvine, W. *Chem. Eng. News* **14 June, 1982**, *59*, 19. See also Gudeman, G. S.; Woods, R. G. *Phys. Rev. Lett.* **1982**, *48*, 1344.
(4) Nobes, R. H.; Radom, L. *J. Chem. Phys.* **1981**, *60*, 1.
(5) Berkowitz, J. *J. Chem. Phys.* **1978**, *69*, 3044.
(6) Momigny, J.; Wankenne, H.; Crier, C. *Int. J. Mass Spectrom. Ion Phys.* **1980**, *35*, 151.
(7) Wesdemiotis, C.; McLafferty, F. W. *Tetrahedron Lett.* **1981**, *22*, 3479.

0002-7863/83/1505-5976$01.50/0